

Reconstructing the Last Interglacial at Summit Greenland: Insights from GISP2

Audrey M. Yau^a, Michael L. Bender^{a,b*}, Alexander Robinson^{c,d,e}, Edward J. Brook^f

^aDepartment of Geosciences, Princeton University, Princeton NJ, 08540 USA ^bInstitute of Oceanology, Shanghai Jiao Tong University, Minhang District, Shanghai, China ^cUniversidad Complutense de Madrid, 28040 Madrid, Spain ^dInstituto de Geociencias, UCM-CSIC, 28040 Madrid, Spain ^ePotsdam Institute for Climate Impact Research, 14473 Potsdam, Germany ^fCollege of Earth, Ocean, and Atmospheric Sciences, Oregon State University, Corvallis OR, 97331 USA

Submitted to Proceedings of the National Academy of Sciences of the United States of America

The Eemian (last interglacial, 130-115 ka) was likely the warmest interglacial of the last 800 ka, with Arctic temperatures up to 6°C above present. We present improved Eemian climate records for central Greenland, reconstructed from ice near the base of the GISP2 ice core. Our record comes from clean, stratigraphically disturbed and isotopically warm ice from 2750-3040 m depth. Ice ages are constrained by measuring CH₄ and d¹⁸O of O₂, and dating the samples given the historical record of these properties from the Greenland NGRIP and NEEM ice cores. d¹⁸O_{ice}, d¹⁵N of N₂, and total air content data for samples dating discontinuously from 128-115 ka indicate a similar elevation change, but different accumulation rate histories, between the GISP2 and NEEM deposition sites. Derived climate histories of temperature, accumulation rate, and relative elevation change are compared to an ensemble of model simulations of the Greenland ice sheet. The coupled climate - ice-sheet model simulations that are most consistent with the reconstructed temperatures from GISP2 and NEEM indicate that the Greenland ice sheet contributed 5.1 m (4.1-6.2 m, 95% credible interval) to global eustatic sea level towards the end of the Eemian. The data and simulations suggest that Greenland did not contribute to anomalously high sea levels at the start of the Eemian, ~127 ka, or to a rapid rise at ~120 ka. However, several unexplained discrepancies remain between the inferred and simulated histories of temperature and accumulation rate at GISP2 and NEEM, as well as between the climatic reconstructions themselves.

Greenland ice sheet | Last interglacial | Ice cores | Sea level rise

Introduction

During the last interglacial (Eemian, 130-115 ka), Arctic summer temperatures were 3-5°C warmer than today (1) and peak global eustatic sea level was likely 6-9 m higher than the present (2). In the next century, due to anthropogenic emissions of greenhouse gases, we face a similar temperature scenario with 2-6°C of northern hemispheric polar warming (3), and a likely initial sea-level rise (by 2100) of 0.3-1.0 m (4), with higher, but uncertain, levels beyond. Certainly there are important differences between the warming and sea-level change observed during the last climatic warm period and future projections, notably the rate at which warming is expected to occur and its spatial pattern. Nevertheless, the Eemian history of the Greenland ice sheet (GrIS) serves as an essential test bed for understanding changes in ice sheets and sea-level rise in response to rising global temperatures.

Ice sheet modeling studies have estimated a wide range of GrIS contributions to sea-level during the Eemian, with simulations producing 0.4-5.5 m of equivalent sea-level rise above the present datum (5). While ice dating to the Eemian or beyond has been observed in six ice cores drilled to the base of the Greenland ice sheet (North GRIP, GRIP, GISP2, Camp Century, Dye 3, and NEEM) (Fig. 1), only the most recently drilled core at NEEM has provided a continuous climate history through the Eemian, with ice as old as 128 ka (6). The NEEM climate record includes data on gas stratigraphy (which defines the timescale), isotopic

temperature, gas trapping depth (from δ¹⁵N of N₂), and total air content (7).

Here, we revisit the climate archive of the deep section of the GISP2 ice core, which contains stratigraphically disturbed layers of ice dating to the last interglacial and beyond (8, 9). The Greenland Ice Sheet Project 2 (GISP2) ice core was drilled to bedrock in 1993, producing a 3053.44 m ice core at Summit, Greenland. Its stratigraphy is continuous to only ~105 ka, or to a depth of ~2750 m (Fig. 1). Below, there are ~290 m with alternating intervals of isotopically warm (heavy δ¹⁸O_{ice}) and cold (light δ¹⁸O_{ice}) ice (10). The warmest of these sections have δ¹⁸O_{ice} values warmer than that of the current interglacial, and gas properties consistent with an Eemian age, indicating that Eemian ice is present near the bed of GISP2 (Fig. 1; 9, 11).

We targeted the warmest disturbed ice, sampling all 48 one-meter sections of the GISP2 ice core between 2760-3040 m depth with δ¹⁸O_{ice} values heavier than -37‰ (Supp. Fig. 1). Measurements of the δ¹⁸O of paleoatmospheric O₂ (δ¹⁸O_{atm}) and the concentration of CH₄ constrain the ages of discrete samples. We then use these dates to improve our understanding of the sequence of events at Summit, Greenland, during the last interglacial. The product is a discontinuous record of isotopic temperatures and ice accumulation rates, as well as the elevation of GISP2 with respect to NEEM, over the Eemian at Summit, Greenland. Finally, we compare model simulations to the reconstructed GISP2 and NEEM records to estimate the regional climatic change and sea-level contribution from the GrIS during the Eemian.

Age Reconstruction

In order to establish a chronology for the sampled sections, we follow earlier work in measuring the δ¹⁸O of paleoatmospheric oxygen (δ¹⁸O_{atm}), and the concentration of CH₄, in the trapped

Significance

This work contributes to the scientific effort focused on developing an accurate assessment of the impact that global warming will have on the Greenland ice sheet. By focusing on the last interglacial, a period warmer than today, we learn about the sensitivity of the ice sheet to climate change. We combine data and model simulations to characterize the Eemian history of the Greenland ice sheet. Our data and insights will be useful for simulating the future of the ice sheet in response to climate change.

Reserved for Publication Footnotes

137
138
139
140
141
142
143
144
145
146
147
148
149
150
151
152
153
154
155
156
157
158
159
160
161
162
163
164
165
166
167
168
169
170
171
172
173
174
175
176
177
178
179
180
181
182
183
184
185
186
187
188
189
190
191
192
193
194
195
196
197
198
199
200
201
202
203
204

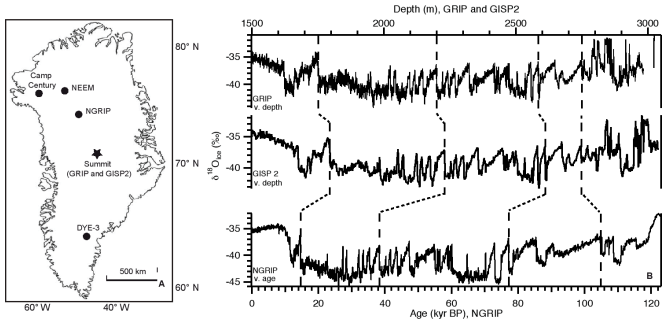


Fig. 1. A: Relevant Greenland ice core drilling sites. B: Comparison of $\delta^{18}\text{O}_{\text{ice}}$ for GRIP, GISP2, and NGRIP ice cores (10, 11). GRIP and GISP2 are plotted on the top axis versus depth and are continuous to ~ 2750 m. NGRIP is plotted on the bottom axis versus age and is continuous to ~ 121 ka. Dotted lines show $\delta^{18}\text{O}_{\text{ice}}$ correlations between cores.

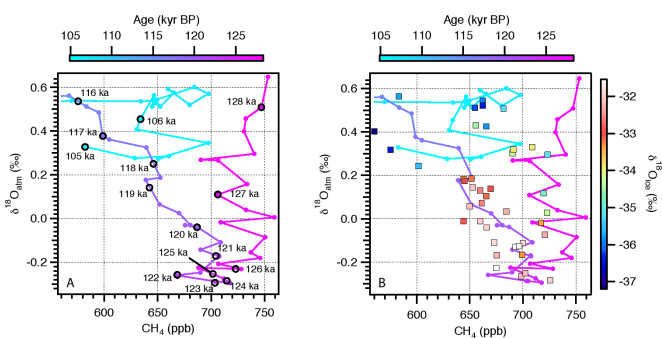


Fig. 2. Reference curves of CH_4 versus $\delta^{18}\text{O}_{\text{atm}}$ color-coded for age. A: Reference curve based on NGRIP (121.1-105 ka; 12) and NEEM (128.2-119.9 ka; 6) CH_4 and $\delta^{18}\text{O}_{\text{atm}}$ data. B: Analyzed sample sections plotted as squares, color-coded for $\delta^{18}\text{O}_{\text{ice}}$ on the reference curve from A.

air bubbles in the ice (8, 9). $\delta^{18}\text{O}_{\text{atm}}$ and CH_4 each vary with time, more or less uniformly, throughout the global atmosphere. We date disturbed ice by determining when, according to existing Greenland and Antarctic ice core records, the atmosphere had the same CH_4 concentration and $\delta^{18}\text{O}_{\text{atm}}$ we observe in a particular sample (Fig. 2). The following ice core records provide the reference $\delta^{18}\text{O}_{\text{atm}}$ and CH_4 stratigraphy: NGRIP from 121.1-105 ka (12); NEEM from 128.2-119.9 ka (6; EDML1 gas age timescale); and EPICA Dome C, dated continuously to ~ 800 ka (13, 14; AICC2012 gas age timescale). In the NEEM dataset, samples with elevated CH_4 and N_2O concentrations are associated with melt layers, and are removed from the reference curve (6; Supp. Fig. 2). Our analysis dates ice at 28 depths in the GISP2 core between 116-128 ka. Details are given in the Supplementary Information.

Coupled climate – ice sheet model

The coupled climate – ice sheet model approach, REMBO-SICOPOLIS, was used to simulate the evolution of the GrIS through the Eemian. Regional climatic conditions over Greenland and the surface mass balance are calculated by the intermediate complexity regional climate model REMBO (15). REMBO includes a computationally efficient 2D atmospheric component and a simplified energy-balance model for calculating the surface mass balance of the ice sheet. The evolution of the ice sheet is calculated via the 3D thermomechanical, shallow-ice approximation ice-sheet model SICOPOLIS (16). SICOPOLIS is driven by the ice surface temperature and surface mass balance fields calculated in REMBO, and in turn it provides ice-sheet thickness and elevation as topographic input back to REMBO. The coupled model is run at 20-km resolution, and it has been shown to simulate the volume and distribution of the present-

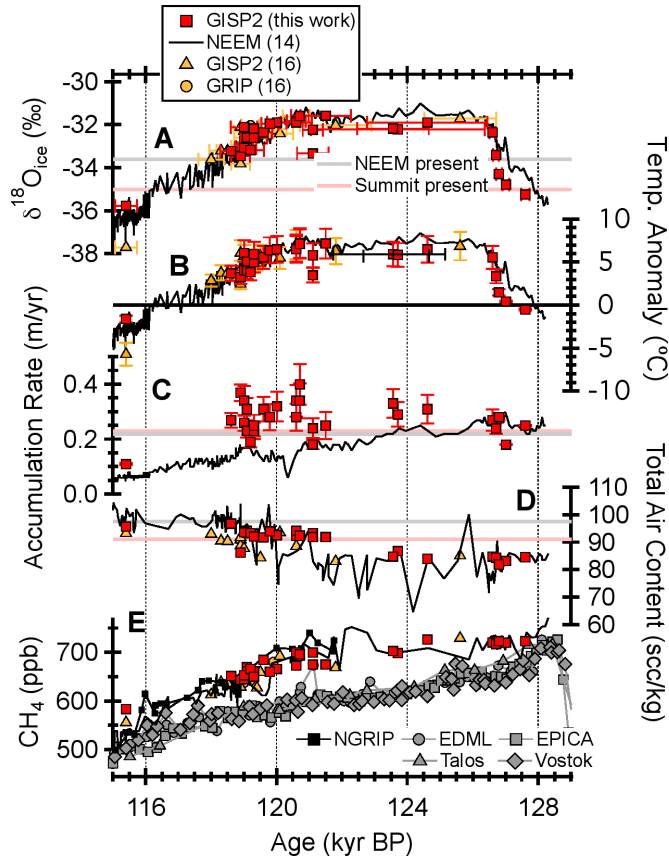


Fig. 3. Summary of data from GISP2 (this work) in red, GRIP and GISP2 in orange (8), and NEEM in black (6) through the last interglacial. A. Reconstructed $\delta^{18}\text{O}_{\text{ice}}$. B. Calculated temperature anomaly relative to the mean of the last millennium for a $dT/d\delta^{18}\text{O}$ relationship of $2.1 \pm 0.5 \text{ }^\circ\text{C } \text{‰}^{-1}$ (6). C. Estimated accumulation rate. D. Reconstructed total air content. E. A comparison of CH_4 data from GISP2 (this work), GRIP and GISP2 (8), NEEM (6), NGRIP (12), EDML (28), EPICA Dome C (13), Talos (29), and Vostok (30).

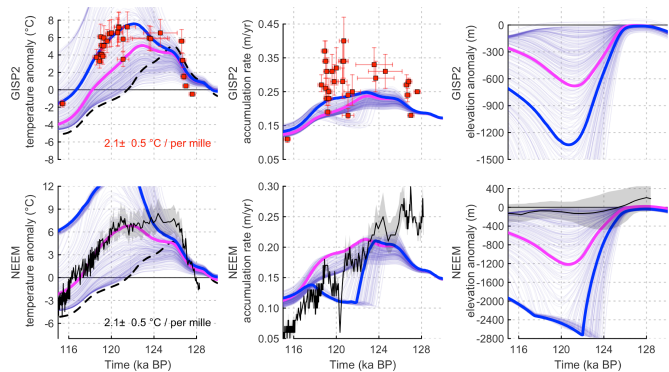


Fig. 4. Simulation output (light blue lines) of the local precipitation-weighted temperature anomaly (left panels), the accumulation rate (center panels) and the elevation (right panels) compared with reconstructions at GISP2 (in red, top row) and NEEM (in black, bottom row; grey shading represents standard error). The most likely simulations when compared to the GISP2 (thick blue lines) and NEEM (thick magenta lines) temperature reconstructions are shown, along with the respective regional summer temperature anomaly forcing in the left panels (dashed black lines).

day ice well (16). Importantly for this study, the model accounts for the albedo-temperature and elevation-melt feedbacks that are active in times of transient ice-sheet evolution, such as during the Eemian. REMBO is driven at the boundaries by monthly

205
206
207
208
209
210
211
212
213
214
215
216
217
218
219
220
221
222
223
224
225
226
227
228
229
230
231
232
233
234
235
236
237
238
239
240
241
242
243
244
245
246
247
248
249
250
251
252
253
254
255
256
257
258
259
260
261
262
263
264
265
266
267
268
269
270
271
272

273
274
275
276
277
278
279
280
281
282
283
284
285
286
287
288
289
290
291
292
293
294
295
296
297
298
299
300
301
302
303
304
305
306
307
308
309
310
311
312
313
314
315
316
317
318
319
320
321
322
323
324
325
326
327
328
329
330
331
332
333
334
335
336
337
338
339
340

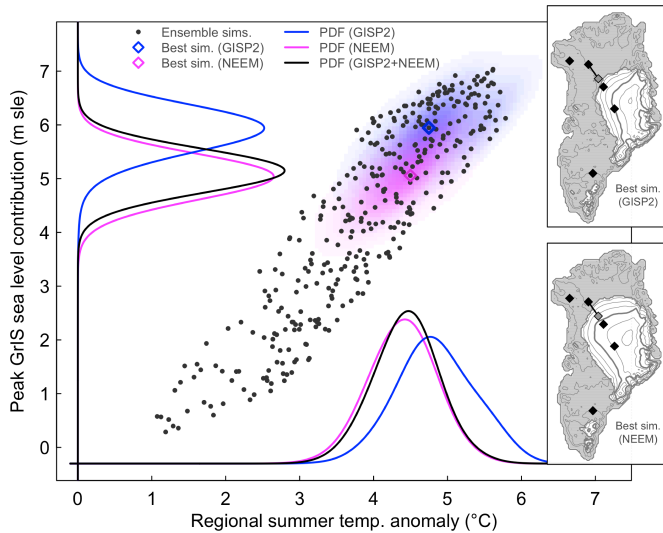


Fig. 5. Simulated maximum GrIS contribution to sea level (m sle) versus the peak regional summer temperature anomaly ($^{\circ}\text{C}$) during the Eemian (black points). Background shading shows the 2D marginal probabilities for GISP2 (blue) and NEEM (magenta) estimated using a weighted kernel density estimate. Probabilities projected onto each variable are shown along with the combined (GISP2+NEEM) estimate. The inset panels show the minimum ice sheet distribution for the best simulation for GISP2 (top panel) and NEEM (bottom panel). The black diamonds on the ice sheet indicate drilling sites, and correspond to sites in Fig. 1. The grey diamond connected to the NEEM point is the estimated upstream deposition site for Eemian age ice.

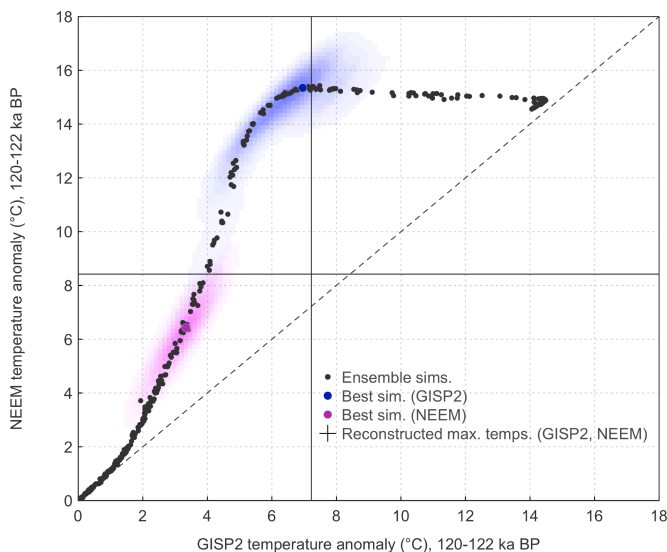


Fig. 6. Simulated average precipitation-weighted temperature anomalies ($^{\circ}\text{C}$) at NEEM versus those of GISP2 during the Eemian for the period 120-122 ka BP (black points). Background shading and the colored points shows the 2D marginal probabilities estimated using a weighted kernel density estimate and the optimal simulations, respectively, for GISP2 (blue) and NEEM (magenta), while the cross indicates the corresponding reconstructed temperature anomalies from the ice cores for this time period. For comparison, the 1-1 relationship of temperature anomalies at NEEM versus GISP2 is shown by the dashed line.

temperature anomalies around Greenland, computed using the CLIMBER-2 earth system model of intermediate complexity in a global glacial cycle simulation from 860 ka to the present driven by greenhouse gas forcing and Milankovitch variability (17).

An ensemble of simulations was performed through the Eemian accounting for parametric uncertainty associated with

the melt model and the sensitivity of precipitation to temperature changes (18), which are dominant factors affecting the transient evolution of the ice sheet. In addition, the positive monthly temperature-anomalies during the Eemian were scaled by a random factor to test a wide range of interglacial temperatures. The ensemble was generated using Latin-Hypercube sampling, where the parameter values were perturbed within a range consistent with present-day constraints (18), and the interglacial temperature anomalies were perturbed to give a peak summer warming range of between about 1-6 $^{\circ}\text{C}$. Prior estimates of parameter weights were assigned to each model version and a posterior likelihood of each simulation was obtained by statistical comparison between the modeled and reconstructed precipitation-weighted temperature anomalies at GISP2 and the NEEM deposition site (see Supplementary Information for details).

Results and Discussion

Climate at Summit, Greenland over the Last Interglacial

Fig. 3 shows climate properties for samples from the clean, disturbed section of the GISP2 core plotted vs. reconstructed age. Also plotted are similar GISP2 data of Suwa *et al.* (8), along with the reconstructed records from NEEM (6). We note that temperature reconstructions are based on precipitation-weighted $\delta^{18}\text{O}_{\text{ice}}$, which is likely biased towards warmer summer months rather than the annual mean temperature (19).

Temperature

We observe a rapid deglacial warming at Summit, similar to that seen in the NEEM core. From 127.6-126.6 ka, GISP2 $\delta^{18}\text{O}_{\text{ice}}$ increases by 2.9‰ from -35.2‰ to -32.3‰ (Fig. 3a). To estimate temperatures, we adopt the temperature- $\delta^{18}\text{O}$ relationship of Vinther *et al.* (20), with the larger uncertainty of NEEM (6), i.e. $dT/d\delta^{18}\text{O}_{\text{ice}} = 2.1 \pm 0.5 \text{ }^{\circ}\text{C } \text{‰}^{-1}$. This value is similar to the present-day spatial relationship of $\delta^{18}\text{O}_{\text{ice}}$ versus temperature, $1.5^{\circ}\text{C } \text{‰}^{-1}$ (21). The $dT/d\delta^{18}\text{O}$ relationship may differ between the Eemian and the Holocene due to changes in seasonality and sources of precipitation (19), as well as topographic feedbacks with a reduced ice sheet size (22), which is reflected in the uncertainty range used here. Using this conversion factor, the $\delta^{18}\text{O}_{\text{ice}}$ change corresponds to a precipitation-weighted warming of $6 \pm 1.5^{\circ}\text{C}$ at Summit over a $\sim 1,000$ year period. After a plateau of several kiloyears, $\delta^{18}\text{O}_{\text{ice}}$ gradually decreases by $\sim 1.5\text{‰}$ from 121.8-118 ka, corresponding to a cooling of $3 \pm 1^{\circ}\text{C}$, again, much like that seen at NEEM.

During the middle of the Eemian, $\delta^{18}\text{O}_{\text{ice}}$ at GISP2 is slightly lower than at NEEM, suggesting that the Summit anomaly was perhaps 1°C lower. At NEEM, highly variable total air content data, along with sharp spikes in CH_4 and N_2O concentrations, indicate frequent surface melt layers between 128-118 ka (6). Such features are not observed at GISP2. Unfortunately, our ability to describe this interval at GISP2 is limited by the paucity of GISP2 and GRIP samples dating between 126-122 ka (this work, 8), which notably corresponds to the period of warmest Eemian temperatures and significant Greenland ice sheet loss (6).

The reconstructed temperature anomaly relative to the mean of the last thousand years is calculated and plotted in Fig. 3b. For reference, present-day values of $\delta^{18}\text{O}_{\text{ice}}$ and temperature are -35‰ and -31 $^{\circ}\text{C}$ for GISP2 and -35‰ and -29 $^{\circ}\text{C}$ for the estimated upstream Eemian NEEM deposition site (6), respectively. Between 126-122 ka, Summit temperatures are estimated to have been 4-8 $^{\circ}\text{C}$ higher than the recent average. This warming reflects the combination of higher regional temperatures and lower ice sheet elevation.

Accumulation Rate

We calculate the accumulation rate as described in the Supplementary Material. Briefly, we calculate temperature from $\delta^{18}\text{O}_{\text{ice}}$ as described above. Next, we calculate gas-trapping depth

409 from $\delta^{15}\text{N}$ of N_2 (23). The equations of Herron and Langway
410 (24) are then solved to calculate the accumulation rate, in units
411 of water-equivalent meters/year, accounting for close off at the
412 observed temperature and gas trapping depth. Estimated accu-
413 mulation rates are shown in Fig. 3c. Accumulation rates decline
414 steadily through the Eemian at NEEM, while they are more
415 variable and do not show a trend at GISP2. Accumulation rates
416 are similar between the two sites at the onset and end of the
417 interglacial period, but reach lower values at NEEM by about
418 ~ 120 ka.

419 **Total air content and elevation**

420 The change in TAC at GISP2 is easily quantified. However
421 at NEEM, the situation is complicated by melting, which leads
422 to anomalously low total air content in many of the samples.
423 The reliable TAC values at NEEM are the highest values except
424 for one anomalously high point at 126 ka. These values are very
425 similar to values at GISP2 throughout the record (Fig. 3d).

426 In principle, total air content (TAC) serves as a proxy for
427 elevation. The premise is that, in ice reaching the close-off
428 depth, open porosity is a function of temperature (7, 25). TAC
429 is then the open porosity at the close-off depth multiplied by the
430 temperature-dependent density of air. Reversing the approach,
431 one can calculate atmospheric pressure during gas trapping from
432 temperature ($\delta^{18}\text{O}_{\text{ice}}$), the empirical relationship between close-
433 off volume and temperature, and the ideal gas law. In addition,
434 Raynaud *et al.* (7) and others (26, 27) identified a link between
435 total air content and local summertime insolation. Accounting for
436 this link, NEEM *et al.* (6) quantified the effect of insolation and
437 estimated that, during the Eemian, elevation at NEEM was within
438 a few hundred meters of the present elevation.

439 The similarity in TAC at NEEM and GISP2 is at least partly
440 due to the fact that the insolation change is nearly identical at
441 these sites. However, the similarity in the records also requires
442 that the magnitude of elevation change between 127-121 ka be
443 similar at the two sites. We have less confidence in *absolute* ele-
444 vations computed from the TAC data (supplementary material),
445 because of the large uncertainty associated with the insolation
446 effect as well as the potential for unquantified regional atmo-
447 spheric pressure changes. Therefore they are not considered in
448 our analysis.

449 In summary, GISP2 data place 3 important constraints on the
450 history of the Greenland ice sheet. First, Summit warmed to the
451 present temperature at ~ 127 ka, and was $\sim 5^\circ\text{C}$ warmer than
452 present between 126-120 ka. Second, Eemian accumulation rates
453 at Summit were $\sim 40\%$ higher than during the Holocene. Third,
454 the elevation and temperature difference between Summit and
455 the deposition site of NEEM was approximately constant during
456 the Eemian.

457 **Data-Model Comparison**

458 We compare output from an ensemble of coupled climate –
459 ice sheet model simulations to the reconstructed temperature,
460 accumulation rate, and elevation change data for Summit and the
461 NEEM upstream deposition location during the Eemian.

462 Several simulations capture either the GISP2 or the NEEM
463 temperature record fairly well, but it is not possible to simulate
464 both well simultaneously (see Fig. 4). The basic problem is that
465 the NEEM-GISP2 elevation difference should not change ap-
466 preciable according to TAC data and the isotopic temperature
467 difference between sites. In our simulations, however, NEEM
468 always declines in elevation more than GISP2, and its isotopic
469 temperature increases more. Given our inability to simultane-
470 ously simulate climate records at both sites, we derive histories
471 of temperature and elevation by independently optimizing prop-
472 erties of the model to fit the NEEM and GISP2 temperature
473 histories.

474 The optimal simulation accounting only for the GISP2 tem-
475 perature reconstruction (Fig. 4, blue lines) produces a peak sea-

476 level contribution from the GrIS of 6 m (Fig. 5). The trajectory
477 of warming during the Eemian is well captured by the simulation,
478 aside from an underestimation of warming early on of approx-
479 imately 2°C . Interestingly, the model fits the data best towards
480 the end of the interglacial when the combination of transient
481 elevation changes and regional climatic forcing leave the model
482 with the most degrees of freedom (see Fig. 6). In this case, the
483 ice sheet is reduced to a small central dome with a reduction
484 in the GISP2 elevation by around 1300 m (Fig. 6, top panel).
485 This solution seems to fail because it predicts the absence of an
486 Eemian ice sheet at the NEEM deposition site inferred by (6).

487 The optimum solution using the NEEM reconstruction (Fig.
488 4, magenta lines) still gives a rather large peak sea-level contri-
489 bution of 5 m (Fig. 5). As with the GISP2-optimal simulation,
490 the initial warming entering the Eemian is underestimated by
491 about 3°C , while the simulation matches the later trajectory of the
492 reconstruction quite well. This simulation implies an elevation re-
493 duction of about 1200 m relative to today at the NEEM deposition
494 site, and a much smaller reduction in elevation at GISP2 of only
495 700 m (Fig. 5, bottom right). This solution also seems deficient. It
496 fails to simulate the constant elevation difference between NEEM
497 and GISP2. It also underestimates the temperature anomaly at
498 GISP2 by $3\pm 1^\circ\text{C}$ between 119-123 ka.

499 The estimated peak regional summer warming (black dashed
500 lines in Fig. 4, prescribed as boundary forcing in the regional
501 climate model) is quite similar in both cases. The combined
502 GISP2 and NEEM posterior likelihood using this forcing gives
503 a best estimate of about 4.5°C regional summer warming, and
504 a 95% credible interval of $3\text{--}5^\circ\text{C}$. This range is quite consistent
505 with previous best estimates of Arctic summer warming during
506 this time period (1). The optimal solutions are also consistent
507 in placing the greatest sea-level contribution late in the Eemian,
508 at ~ 121 ka (see Supplementary Fig. 6), which is also when the
509 regional summer temperature falls below the modern value in
510 the simulations. At its minimum, the resulting GrIS is reduced
511 to a rather small northern dome and some sporadic ice-covered
512 regions in the South (Fig. 5 insets).

513 The initial rise in temperature seen in all of the simulations
514 is predominantly due to the background regional warming. These
515 high temperatures initiate melting and a reduction of the volume
516 and area of the ice sheet. Ice dynamics dictate that there must
517 be a lag between the onset of melting and the volume reduction,
518 since the former can only occur at a limited rate. By 125 ka,
519 regional temperatures begin to fall. In the both optimum simu-
520 lations, Summit and NEEM remain warm until ~ 122.5 ka due to
521 declining elevations, which counteract the regional cooling signal
522 (see Fig. S 5 for the Summit-optimal case). At around 122-121
523 ka, the simulated ice volume reaches its minimum, elevations
524 stabilize and the background cooling again dominates the local
525 temperature signal.

526 There are a number of features that the optimum models
527 fail to capture. First, and most apparent, is the magnitude of the
528 early temperature anomalies of about $6\text{--}8^\circ\text{C}$ at both GISP2 and
529 NEEM. This poor fit is in stark contrast to the rather good fit
530 later in the Eemian. It is unlikely that the regional temperature
531 forcing was larger than simulated here, because it would result
532 in even faster ice-sheet melt and an even worse overall fit with
533 the reconstructions. Furthermore, the sensitivity of $\delta^{18}\text{O}_{\text{ice}}$ to
534 temperature may not always be within the range $2.1 \pm 0.5^\circ\text{C}/\text{‰}$.
535 Temporal deviations away from this factor may account for the
536 misfit between inferred and simulated temperature histories early
537 in the Eemian. In general, the use of a constant conversion factor
538 in time could in fact erroneously suggest a constant temperature
539 difference between GISP2 and NEEM and should also be re-
540 garded cautiously.

541 Second, the optimum simulation predicts maximum accu-
542 mulation rates at GISP2 similar to the Holocene, while the

545 data suggest that rates were considerably higher (Fig. 4). Gas
546 trapping depths (based on the gravitational enrichment of N_2)
547 are temperature-dependent, and they were similar during the
548 Holocene and Eemian. However, Eemian isotopic temperatures
549 were much warmer. Warmer temperatures imply higher accumu-
550 lation rates to prevent shoaling of the trapping depth. The model
551 does not reproduce the NEEM accumulation rate record well.
552 Thus, it may be that simulated SLR contributions are slightly
553 overestimated as a result of mismatches between inferred and
554 simulated accumulation rates, although the work of Cuffey and
555 Marshall (31) suggest that the bias would be less than ~ 0.5 m.

556 The poor fit with some aspects of the reconstructions may
557 imply that a more detailed modeling approach is needed. The
558 dominant driver of GrIS changes during the Eemian is changes
559 in surface mass balance and, thus, changes in climate. Here we
560 applied a spatially constant temperature anomaly to force our
561 simple regional climate model, which could bias the comparison
562 between the two cores if in reality the climate showed more
563 complex patterns of anomalies. Nonetheless, the overall sensi-
564 tivity of the ice sheet to large-scale climate changes (as well as
565 its uncertainty) should be well represented by our ensemble of
566 simulations, which gives confidence to the estimated ice-sheet
567 retreat and sea-level contribution.

568 Optimizing the Greenland SLR contribution against both
569 temperature records suggests that the GIS contribution was 5.1
570 meters (4.1-6.2 m, 95% credible interval). Given regional summer
571 temperature anomalies in the range of 3-5°C, a substantial ele-
572 vation reduction at both sites is required to achieve and sustain
573 the high Eemian temperatures implied by the $\delta^{18}O_{ice}$ data. If,
574 instead, the minimum elevations at these sites would have been
575 comparable to today, the regional temperature anomaly required
576 to reproduce the $\delta^{18}O_{ice}$ signal would be closer to 8-10°C (see S.
577 Fig. 5). Such warm values would be inconsistent with other Arctic
578 paleo archives (32), as well as global climate model simulations
579 for the period (33) that show no more than 0.5-6.5°C summer
580 warming. In addition, summer temperature anomalies of 8-10°C
581 would melt the GrIS completely in even the most conservative
582 members of the model ensemble. Such a fate would obviously be
583 inconsistent with the existence of Eemian-age ice at the base of
584 the GrIS. Invoking a lower sensitivity of T to $\delta^{18}O_{ice}$, say 1.5‰/‰,
585 diminishes the magnitude of the temperature change, but does
586 not change the basic picture.

587 The data-model comparison reveals a key challenge to our
588 understanding of the climatic reconstructions from the two sites.
589 Both the TAC and $\delta^{18}O_{ice}$ data indicate that changes in eleva-
590 tion and temperature in both cores were similar throughout the
591 Eemian (Fig. 3, Fig. 6). However, the simulations indicate that for
592 only moderate warming at GISP2 of less than 2°C, the NEEM
593 temperature already becomes significantly higher (Fig. 6). This
594 is not surprising. The NEEM deposition site sits closer to the
595 margin in a rather arid zone of the ice sheet, where a small amount
596 of warming leads to ice loss in the region. Therefore, it is not
597 possible to obtain high enough temperatures to match the GISP2
598 reconstruction while maintaining low enough temperatures to
599 match the NEEM reconstruction. This apparent paradox could
600 potentially be resolved if the location of the NEEM deposition
601 site changed much more dynamically during the Eemian than has
602 been assumed until now.

603 Implications for the source of Last Interglacial sea-level rise

604 Our optimum simulations give a maximum Greenland contribu-
605 tion of 5 and 6 m to Eemian sea-level rise, using NEEM
606 and GISP2 respectively. The 95% credible uncertainty interval
607 supports a large contribution from Greenland of at least 3.9 m
608 (based on the more conservative NEEM-optimal comparison),
609 while the joint PDF gives a range of 4.1-6.2 m. This range is
610 considerably higher than most recent estimates (5). Our model
611 includes an explicit representation of the albedo-melt feedback,

612 as well as the effect of changing insolation on surface mass
613 balance, which could explain a greater sensitivity here to Eemian
614 climate changes than seen in previous studies (e.g., 34, 35). Helsen
615 et al. (36) estimate the maximum sea-level contribution from
616 Greenland to be between 1.2-3.5 m, using a regional climate
617 model coupled to an ice-sheet model via a full energy balance
618 model at the surface. Their results are quite consistent with the
619 TAC-based reconstruction of small elevation changes at NEEM
620 during the Eemian (6). However at both the Summit and at
621 NEEM, the modeled temperature anomaly is underestimated by
622 several degrees compared to the reconstructions. In contrast, we
623 find that the simulations with significant reductions in elevation
624 at both Summit and NEEM are most consistent with the isotopic
625 temperature reconstructions.

626 According to the data, GISP2 and NEEM initially reach
627 temperatures comparable to preindustrial levels only at ~ 127 ka.
628 In the simulations, Greenland first begins contracting below its
629 present volume at ~ 126 ka. The maximum Greenland sea-level
630 contribution is attained in the most likely simulations at ~ 121 ka,
631 just as Greenland temperatures start to fall below preindustrial
632 levels. Meanwhile, according to Dutton *et al.* (5) and O'Leary
633 *et al.* (37), global sea level was already elevated by 3-6 m above
634 the modern level at 127 ka. East Antarctica warmed to Holocene
635 temperatures by ~ 131 ka, and reached a temperature maximum
636 shortly thereafter (38). Therefore, Antarctica is a much stronger
637 candidate than Greenland as the source of elevated sea level early
638 in the Eemian (see also 38). Our data suggest that Greenland
639 contributed to elevated sea level at the end of the Eemian (~ 121
640 ka) and its maximum contribution was likely not coeval with that
641 of Antarctica.

642 Finally, at neither Summit nor NEEM do we observe any
643 evidence for a collapse of the GrIS that would correspond to the
644 sea-level rise at 120 ka inferred from Western Australian coral
645 samples (37). If there was such a collapse its source must have
646 been East or West Antarctica.

647 Conclusions

648 We have presented a reconstructed history of temperature, accu-
649 mulation rate, and elevation change at Summit, Greenland during
650 the Eemian. The $\delta^{18}O_{ice}$ data from the GISP2 ice core indicate
651 that Summit warmed rapidly through the deglacial, with local,
652 precipitation-weighted temperatures rising to ~ 4 -8°C above the
653 modern millennial average between 128-126 ka. The local tem-
654 perature remained high throughout the Eemian until ~ 121 ka,
655 even as the regional temperature likely fell due to lower insola-
656 tion. This sustained plateau in Summit temperature results from
657 the sum of regional temperature and local elevation effects on
658 $\delta^{18}O_{ice}$. Accumulation rates remain high and variable through the
659 early and mid-Eemian at Summit, which contrasts with the steady
660 decline in accumulation rates observed at NEEM. Total air con-
661 tent data indicate that the elevation difference between GISP2
662 and NEEM remained relatively constant during the Eemian.

663 In the data and in the simulations, Greenland surpassed its
664 preindustrial temperature at ~ 127 ka. Both the data and the
665 simulations suggest that Greenland was not responsible for the
666 elevated global sea level observed at this time. By 121 ka, however,
667 we estimate that the Greenland ice sheet contributed 5.1 m (4.1-
668 6.2 m, 95% credible interval) to excess sea-level rise relative to the
669 modern. There is no evidence, however, that Greenland melting
670 contributed to the inferred rapid rise in sea-level rise at 120 ka.
671 Finally, while our results imply a large contribution of Greenland
672 to sea level during this time, discrepancies between the simulated
673 and observed relative changes between the ice cores remain to be
674 explained. In addition, of course, this and similar studies are also
675 limited by the fidelity of the climate and ice sheet models used in
676 the simulations.

677 Methods

681
682
683
684
685
686
687
688
689
690
691
692
693
694
695
696
697
698
699
700
701
702
703
704
705
706
707
708
709
710
711
712
713
714
715
716
717
718
719
720
721
722
723
724
725
726
727
728
729
730
731
732
733
734
735
736
737
738
739
740
741
742
743
744
745
746
747
748

Air Analysis

CH₄ and total air content measurements were conducted at Oregon State University following analytical methods detailed in Grachev *et al.*, Mitchell *et al.* (39, 40), and Rosen *et al.* (41). Out of 48 samples, we excluded two in which replicate subsamples differed by more than 25 ppb. We also eliminated five samples with likely excess concentrations of CH₄ (see Results). The standard deviation of replicates for the remaining 41 samples was ± 3 ppb. An inter-laboratory comparison of Holocene CH₄ data shows good agreement and validates comparisons of CH₄ concentrations between the NEEM and NGRIP (University of Bern, 15) and GISP2 (Oregon State University, 43, where our samples were analyzed) ice cores. The early Holocene CH₄ average from OSU is ~ 736 ppb, and from Bern is ~ 735 ppb. During the Younger Dryas, the CH₄ average from OSU, is 503 ppb; that of Bern is 506 ppb.

$\delta\text{O}_2/\text{N}_2$, $\delta\text{Ar}/\text{N}_2$, $\delta^{15}\text{N}$, and $\delta^{18}\text{O}_{\text{atm}}$ of trapped air was measured at Princeton University using an adapted extraction and equilibration technique based on Emerson *et al.* and Dreyfus *et al.* (42, 43). In these extractions,

1. Clark PU, Huybers P (2009) GLOBAL CHANGE Interglacial and future sea-level. *Nature* 462(7275):856-857.
2. Kopp RE, Simons FJ, Mitrovica JX, Maloof AC, Oppenheimer M (2009) Probabilistic assessment of sea-level during the last interglacial stage. *Nature* 462(7275):863-U851.
3. IPCC, 2013: Annex I: Atlas of Global and Regional Climate Projections [van Oldenborgh GJ, *et al.* (eds.)]. In: Climate Change 2013: The Physical Science Basis. Contribution of Working Group I to the Fifth Assessment Report of the Intergovernmental Panel on Climate Change [Stocker TF, *et al.* (eds.)]. Cambridge University Press, Cambridge, United Kingdom and New York, NY, USA.
4. IPCC, 2013: Annex II: Climate System Scenario Tables [Prather M, *et al.* (eds.)]. In: Climate Change 2013: The Physical Science Basis. Contribution of Working Group I to the Fifth Assessment Report of the Intergovernmental Panel on Climate Change [Stocker TF, *et al.* (eds.)]. Cambridge University Press, Cambridge, United Kingdom and New York, NY, USA.
5. Dutton A, *et al.* (2015) Sea-level rise due to polar ice-sheet mass loss during past warm periods. *Science* 349(6244):aaa4019.
6. NEEM (2013) Eemian interglacial reconstructed from a Greenland folded ice core. *Nature* 493(7433):489-494.
7. Raynaud D, *et al.* (2007) The local insolation signature of air content in Antarctic ice. A new step toward an absolute dating of ice records. *Earth Planet. Sci. Lett.* 261:337-349.
8. Suwa M, von Fischer JC, Bender ML, Landais A, Brook EJ (2006) Chronology reconstruction for the disturbed bottom section of the GISP2 and the GRIP ice cores: Implications for Termination II in Greenland. *J. Geophys. Res.-Atmos.* 111: 10.1029/2005JD006032.
9. Chappellaz J, Brook E, Blunier T, Malaize B (1997) CH₄ and delta O-18 of O-2 records from Antarctic and Greenland ice: A clue for stratigraphic disturbance in the bottom part of the Greenland Ice Core Project and the Greenland Ice Sheet Project 2 ice cores. *J. Geophys. Res.-Oceans* 102:26547-26557.
10. Grootes PM, Stuiver M, White JWC, Johnsen S, Jouzel J (1993) Comparison of oxygen-isotope records from the GISP2 and GRIP Greenland ice cores. *Nature* 366(6455):552-554.
11. Johnsen SJ, *et al.* (2001) Oxygen isotope and palaeotemperature records from six Greenland ice-core stations: Camp Century, Dye-3, GRIP, GISP2, Renland and NorthGRIP. *J. Quat. Sci.* 16(4):299-307.
12. Capron E, *et al.* (2010) Synchronising EDML and NorthGRIP ice cores using delta O-18 of atmospheric oxygen (delta O-18(atm)) and CH4 measurements over MIS5 (80-123 kyr). *Quat. Sci. Rev.* 29:222-234.
13. Loulergue L, *et al.* (2008) Orbital and millennial-scale features of atmospheric CH4 over the past 800,000 years. *Nature* 453(7193):383-386.
14. Dreyfus GB (2008) Dating an 800,000 year Antarctic ice core record using the isotopic composition of trapped air. Thesis Dissertation. Princeton University Press.
15. Greve R (1997) A continuum-mechanical formulation for shallow polythermal ice sheets. *Philos. Trans. R. Soc. London. Ser. A Mathematical, Phys. Eng. Sci.* 355(1726):921-974.
16. Robinson A, Calov R, Ganopolski A (2010) An efficient regional energy-moisture balance model for simulation of the Greenland Ice Sheet response to climate change. *Cryosph.* 4(2):129-144.
17. Ganopolski A, Calov R (2011) The role of orbital forcing, carbon dioxide and regolith in 100 kyr glacial cycles. *Clim. Past* 7:1415-1425.
18. Robinson A, Calov R, Ganopolski A (2012) Multistability and critical thresholds of the Greenland ice sheet. *Nat. Clim. Chang.* 2(4):429-432.
19. van de Berg WJ, van den Broeke MR, van Meijgaard E, Kaspar F (2013) Importance of precipitation seasonality for the interpretation of Eemian ice core isotope records from Greenland. *Clim. Past* 9:1589-1600.
20. Vinther BM, *et al.* (2009) Holocene thinning of the Greenland ice sheet. *Nature* 461(7262):385-388.
21. Johnsen SJ, Dansgaard W, White JWC (1989) The origin of Arctic precipitation under present and glacial conditions. *Tellus Ser. B-Chem. Phys. Meteorol.* 41:452-468.
22. Merz N, Born A, Raible CC, Fischer H, Stocker TF (2014) Dependence of Eemian Greenland temperature reconstructions on the ice sheet topography. *Clim. Past* 10:1221-1238.
23. Sowers T, Bender ML, Raynaud D (1989) Elemental and isotopic composition of occluded O₂ and N₂ in polar ice. *J. Geophys. Res.-Atmos.* 94:5137-5150.
24. Herron MM, Langway CC (1980) Firn Densification - An empirical model. *J. Glaciology.* 25(93):373-385.
25. Martinerie P, Raynaud D, Etheridge DM, Barnola JM, Mazaudier D (1992) Physical and climatic parameters which influence the air content in polar ice. *Earth Planet. Sc. Lett.* (112):1-13.

~ 20 g of ice were used, and the equilibrating time of the headspace and melt water was 1 hr. The analytical uncertainty based on the standard deviations of modern air standards (air taken directly from the roof of the Princeton University Geosciences building in New Jersey, USA; $n = 28$) for $\delta\text{O}_2/\text{N}_2$ is $\pm 0.49\text{‰}$, for $\delta\text{Ar}/\text{N}_2$ is $\pm 0.29\text{‰}$, for $\delta^{15}\text{N}$ is $\pm 0.02\text{‰}$, and for $\delta^{18}\text{O}$ of O₂ is $\pm 0.04\text{‰}$. The paleoatmospheric $\delta^{18}\text{O}$, $\delta^{18}\text{O}_{\text{atm}}$, is equal to $\delta^{18}\text{O}$ of O₂ corrected for gravitational fractionation: $\delta^{18}\text{O}_{\text{atm}} = \delta^{18}\text{O} - 2.01 * \delta^{15}\text{N}$. The standard deviation for $\delta^{18}\text{O}_{\text{atm}}$ of modern air standards is $\pm 0.04\text{‰}$.

Acknowledgements.

This work was supported by grants PLR 1107343 and 1107744 from the U.S. National Science Foundation. A.R. was funded by the Marie Curie 7th Framework Programme (Project PIEF-GA-2012-331835, EURICE) and the Spanish Ministerio de Economía y Competitividad (Project CGL2014-59384-R, MOCCA). We thank the members of the National Ice Core Laboratory for their support in recovering samples from the ice core archive. We are grateful to Mahé Perrette for help with the statistical analysis.

26. Eicher O, Baumgartner M, Schilt A., Schmitt J, Schwander J, Stocker TF, Fischer H (2015) Climatic and insolation control on the high-resolution total air content in the NGRIP ice core. *Clim. Past Discuss.* 11,5509-5548.
27. Lipenkov V, Raynaud D, Loutre M, Duval P (2011) On the potential of coupling air content and O₂/N₂ from trapped air for establishing an ice core chronology tuned on local insolation. *Quat. Sci. Rev.* 30:3280-3289.
28. Schilt A, *et al.* (2010) Atmospheric nitrous oxide during the last 140,000 years. *Earth Planet. Sci. Lett.* 300:33-43.
29. Buiron D, *et al.* (2011) TALDICE-1 age scale of the Talos Dome deep ice core, East Antarctica. *Clim. Past* 7(1):1-16.
30. Petit JR, *et al.* (1999) Climate and atmospheric history of the past 420,000 years from the Vostok ice core, Antarctica. *Nature* 399(6735):429-436.
31. Cuffey KM, Marshall SJ (2000) Substantial contribution to sea level rise during the last interglacial from the Greenland Ice Sheet. *Nature* 404: 591-594.
32. Capron E, *et al.* (2014) Temporal and spatial structure of multi-millennial temperature changes at high latitudes during the Last Interglacial. *Quat. Sci. Rev.* 103:116-133.
33. Bakker P, *et al.* (2013) Last interglacial temperature evolution - a model inter-comparison. *Clim. Past* 9(2):605-619.
34. Quiquet, A, Ritz C, Punge HJ, Salas y Melia D (2013) Greenland contribution to sea level rise during the last glacial period: a modeling study driven and constrained by ice core data. *Clim. Past* 9: 353-366.
35. Stone EJ, Lunt DJ, Annan JD, Hargreaves JC (2013) Quantification of the Greenland ice sheet contribution to Last Interglacial sea level rise. *Clim. Past* 9: 621-639.
36. Helsen MM, van der Berg WJ, van de Wal RSW, van den Broeke MR, Oerlemans J (2013) Coupled regional climate-ice-sheet simulation shows limited Greenland ice loss during the Eemian. *Clim. Past* 9: 1773-1788.
37. O'Leary MJ, *et al.* (2013) Ice sheet collapse following a prolonged period of stable sea-level during the last interglacial. *Nature Geoscience* 6:796-800.
38. Steig EJ, *et al.* (2015) Influence of West Antarctic Ice Sheet collapse on Antarctic surface climate. *Geophys. Res. Lett.* 42(12):10.1002/2015GL063861.
39. Grachev AM, Brook EJ, Severinghaus JP, Piasias NG (2009) Relative timing and variability of atmospheric methane and GISP2 oxygen isotopes between 68 and 86 ka. *Glob. Biogeochem. Cycle* 23:10.1029/2008GB003330.
40. Mitchell LE, Brook EJ, Sowers T, McConnell JR, Taylor K (2011) Multidecadal variability of atmospheric methane, 1000-1800 CE. *J. Geophys. Res.-Biogeosci.* 116: 10.1029/2010JG001441.
41. Rosen JL, *et al.* (2014) An ice core record of near-synchronous global climate changes at the Bolling transition. *Nature Geoscience* 7(6):459-463.
42. Emerson S, Quay PD, Stump C, Wilbur D, Schudlich R (1995) Chemical tracers of productivity and respiration in the subtropical Pacific Ocean. *J. Geophys. Res.-Oceans* 100:15873-15887.
43. Dreyfus GB, *et al.* (2007) Anomalous flow below 2700 m in the EPICA Dome C ice core detected using delta O-18 of atmospheric oxygen measurements. *Clim. Past* 3(2):341-353.
44. Bender ML, Sowers T, Lipenkov V (1995) On the concentrations of O-2, N-2, and Ar in trapped gases from ice cores. *J. Geophys. Res.-Atmos.* 100:18651-18660.
45. Bender ML, Burgess E, Alley RB, Barnett B, Clow GD (2010) On the nature of the dirty ice at the bottom of the GISP2 ice core. *Earth Planet. Sci. Lett.* 299:466-473.
46. Souchez R, Janssens L, Lemmens M, Stauffer B (1995) Very-low oxygen concentration in basal ice from Summit, Central Greenland. *Geophys. Res. Lett.* 22(15):2001-2004.
47. Seierstadt I, *et al.* (2014) Consistently dated records from the Greenland GRIP, GISP2 and NGRIP ice cores for the past 104 ka reveal regional millennial-scale $\delta^{18}\text{O}$ gradients with possible Heinrich event imprint. *Quat. Sci. Rev.* 106:29-46.
48. Raynaud D, Chappellaz J, Ritz C, Martinerie P (1997) Air content along the Greenland Ice Core Project core: A record of surface climatic parameters and elevation in central Greenland. *J. Geophys. Res.-Oceans* 102:26607-26613.
49. Martinerie P, *et al.* (1994) Air content paleo record in the Vostok ice core (Antarctica): A mixed record of climatic and glaciological parameters, *J. Geophys. Res.* 99:10565-10576.
50. Baumgartner M *et al.* (2012) High-resolution inter-polar difference of atmospheric methane around the Last Glacial Maximum. *Biogeosciences* 9: 3961-3977.

749
750
751
752
753
754
755
756
757
758
759
760
761
762
763
764
765
766
767
768
769
770
771
772
773
774
775
776
777
778
779
780
781
782
783
784
785
786
787
788
789
790
791
792
793
794
795
796
797
798
799
800
801
802
803
804
805
806
807
808
809
810
811
812
813
814
815
816